

Monte Carlo simulation of segregation in ceramic thin films: Comparison of the MgO/MnO {1 0 0} and {2 1 0} surfaces

John A. Purton^{a,*}, Neil L. Allan^b

^a*CCLRC, Daresbury Laboratory, Warrington WA4 4AD, UK*

^b*School of Chemistry, University of Bristol, Cantock's Close, Bristol BS8 1TS, UK*

Available online 20 July 2006

Abstract

A Monte Carlo exchange technique is used to study segregation in thin ceramic films with application to the $\text{Mg}_{1-x}\text{Mn}_x\text{O}$ {1 0 0} and {2 1 0} surfaces. Unlike previous atomistic simulations of segregation the method is not restricted to the dilute limit. For all compositions studied ($0 \leq x \leq 1$), the surface is Mn^{2+} rich; the occupancy of sites by Mn^{2+} decreases rapidly with depth. The ratio of the number of Mn^{2+} to Mg^{2+} ions at the surface decreases as a function of temperature. Segregation is greater at {2 1 0} than {0 0 1} surface, consistent with the relative difference in surface energies. Surface concentrations as a function of temperature and film composition are determined directly from the simulations. The calculated enthalpies of segregation are strongly dependent on the surface coverage, particularly for low Mn^{2+} mole fractions.

© 2006 Elsevier B.V. All rights reserved.

PACS: 02.70.Uu

Keywords: A1. Computer simulation; A1. Segregation; B1. Oxides

1. Introduction

The last decade has seen the emergence of tremendous interest in the properties of thin films, stimulated by their commercial potential in a wide range of products including sensors, catalysts, optoelectric devices and magnetic storage devices [1]. Moreover, the last decade has witnessed an emergence of interest in semiconductor nanoparticles which exhibit properties that differ from those of the bulk material; such particles include quantum dots (QD), quantum wells and quantum boxes. For example, the fabrication of (opto)electronic circuits via the self-assembly of QDs is often cited as a potential commercial benefit. Electronic circuit components are usually based on junctions, either between regions of different doping (p–n junctions) or between materials having different band energies (heterojunctions). As band energy changes with particle size, a simple method of obtaining heterojunctions

using QDs would be to construct arrays composed of particles of a single material but of various sizes. Unfortunately controlling the assembly of different sized particles in order to achieve a well-defined circuit architecture is extremely challenging. An alternative strategy is to facilitate the self-assembly of QDs via the introduction of chemical heterogeneity. Thus, the electronic and optical properties of CdSe can be modified by doping with Te to form either homogeneous $\text{CdSe}_{1-x}\text{Te}_x$ or $\text{CdSe}_{1-x}\text{Te}_x$ nanoparticle mixtures [2]. The design of novel devices requires control over both the mechanical and the chemical properties of the film/interface and thus requires an understanding of the behaviour of both the host and the impurity cations or anions. The surface/interface always provides a different elastic and electrostatic environment to that of the bulk, and so there is a free energy difference between the energy associated with any defect, including an impurity, in the bulk and at the surface. Impurities are thus driven to or from the surface/interface. Somewhat surprisingly, atomistic simulations of oxide surfaces have largely concentrated on the growth of thin films [3,4] while recent simulations of thermodynamic

*Corresponding author. Tel.: +44 1925 603785; fax: +44 1925 603100.

E-mail addresses: j.a.purton@dl.ac.uk (J.A. Purton),
n.l.allan@bris.ac.uk (N.L. Allan).

properties of ionic/semiconductor mixtures and solid solutions have tended to be directed more towards disorder and phase equilibria in the bulk [5,6]. In this paper, we report on the results of Monte Carlo (MC) simulations to determine the structure and thermodynamic properties of thin films comprised of a mixture of ionic materials. In addition, we explore the possibility of creating nanosized domains taking advantage of surface segregation. Here, we compare MgO(100)–MnO(100) and MgO(210)–MnO(210) thin films on MgO(100) and MgO(210) substrates, respectively. The magnitude of the size difference between the larger Mn^{2+} and the smaller Mg^{2+} ion (the difference in ionic radii, 0.83 and 0.72 Å, respectively, in 6-fold coordination) is neither so small that an essentially ideal solution is formed at all compositions and temperatures, nor so large that there is always complete segregation by one cation under all conditions of interest. Computer simulations on different structures allow us to explore the rôle of surface terminations on the heat of segregation. Moreover, the bulk MgO–MnO system has been studied in detail using both MC and direct free-energy minimization [7] and the short-range potentials have been tested robustly by several groups.

2. Methodology

A number of atomistic simulation studies have examined the enthalpy of segregation of trace elements both in binary oxides [8–10] and in more complex oxides [11] such as $\text{La}_2\text{CuO}_4/\text{Nd}_2\text{CuO}_4$. These suggest coverage-independent enthalpies of segregation are a crude approximation, except at very low coverages. However these studies determined enthalpies of segregation via energy minimisation only in the static limit (i.e., at 0 K and neglecting lattice vibrations) of small ordered surface supercells in which a periodic ‘superlattice’ of impurity ions was introduced at the surface plane. Enthalpies of segregation were calculated from the energies of these structures, together with the energy of the pure surface and point defect energies associated with isolated impurity ions in the bulk. These calculations thus apply only to crystals containing low levels of bulk impurity. A single surface-layer ordering for each coverage has generally been assumed. Another technique for calculating surface segregation in cubic oxides [12] is based on an effective atom method (a variant of mean-field treatment), in which interactions between neighbouring sites depend on the average concentration of both species in the system. Since in the bulk related mean field treatments [5] give enthalpies of mixing that are largely in excess of the values obtained taking local structural relaxation and clustering explicitly into account, we have chosen not to use such an approach here.

The basis for all our calculations is the well-known MC method modified for surfaces, thin films and interfaces of mixtures of ionic materials. The calculations explicitly include the effects of temperature, full surface relaxation

and are not restricted to the dilute limit. Large supercells are required for statistical analysis and mean that we have far more flexibility in possible arrangements of the atoms at the surface rather than assuming a small number of highly periodic arrangements. No assumptions are made as to the positions of the impurity/dopant atoms in the surface supercell corresponding to a particular coverage. Surface concentrations as a function of temperature are determined directly from the simulations without assuming any particular isotherm and we are able to examine straightforwardly order–disorder at the surface of the film both as a function of film composition and temperature.

The computational technique has been described in a previous paper [13]. However, for completeness it will be briefly discussed below. All calculations are based on an ionic model using two-body potentials to represent short-range forces [14]. The surfaces are assumed to be planar, semi-infinite and periodic in two dimensions [15]. The total long-range electrostatic energy is evaluated using the Parry summation [15]. The particular set of non-Coulombic interaction potentials employed is that of Lewis and Catlow [16] first introduced in their study of the parent oxides, and used here with a cut-off of 10 Å. No mean-field approximations are made. We have used this previously in studies of bulk MnO–MgO solid solutions [17] and the resulting phase diagram, calculated using exchange MC and the semigrand canonical ensemble, is in good agreement with experiment with a consolute temperature of ≈ 1150 K [18].

In simulations of non-stoichiometric ionic materials and solid solutions using ‘standard’ MC, kinetic barriers prevent sampling the whole of the configurational space since almost always only one cation arrangement—the initial configuration—is sampled. We have described elsewhere [5] Monte Carlo exchange (MCX) simulations in which both the atomic configuration and the atomic coordinates of all the atoms are changed. Each calculation consisted of an equilibration of 1.5×10^4 cycles followed by four simulations that combined both equilibration and production parts. The surface concentration presented is an average of the four production runs. The equilibration and production parts of each simulation consisted of 5×10^3 and 10^4 cycles, respectively. We define a cycle to include both the attempted displacement of all the ions and an exchange of ionic configuration. Allowing random moves of randomly selected atoms takes account of both surface relaxation and vibrational effects. To determine whether the change is accepted or rejected, the usual Metropolis algorithm is applied [19]. The maximum change in the atomic displacement for each ionic species has a variable r_{max} , its magnitude is adjusted automatically during the simulation to maintain an acceptance/rejection ratio of approximately 0.5. Changes in ionic configuration are attempted by exchanging the position of a Mn^{2+} ion and a Mg^{2+} ion, both chosen at random. Again, the Metropolis algorithm is used to accept or reject any attempted exchange. In order to represent the deposition of

a film on an inert substrate, only the atoms within the four layers of the thin film were allowed to intermix. This allows us to discriminate between the effects of the substrate on the overlying film and processes operating within the film. The number of atoms in each layer of the film is monitored as the simulation proceeds, and thus x_s is an average of values obtained during the simulation.

3. Results and discussion

All simulations were performed on a hypothetical thin film consisting of four layers of composition $\text{Mg}_{1-x}\text{Mn}_x\text{O}$ that was supported on a MgO substrate. It was assumed that the thin film and substrate have the same surface structure, i.e. $\{100\}$ or $\{210\}$. In order to describe the surface segregation, the surface is ‘divided’ into layers. Surface unit cells and the stacking sequences perpendicular to the surfaces are displayed in Fig. 1. The $\{001\}$ surface is planar and each surface cation/anion is surrounded by five nearest neighbours (Fig. 1). In contrast, Fig. 1b displays the $\{210\}$ surface, in which ridges of alternating O^{2-} and M^{2+} ions run along the $[010]$ direction. The outermost (layer 1) cations and anions are both four coordinate and

the ions in the second layer have five nearest neighbours. The calculations were performed on a thin film comprising 576 and 512 ions for the $\{100\}$ and $\{210\}$ thin films, respectively (i.e., $12 \times 12 \times 4$). The substrate was comprised of $12 \times 12 \times 20$ MgO unit cells. The lattice parameters for the MgO substrate were held fixed at those levels obtained in a previous bulk MC simulation using NPT ensemble at the appropriate temperature.

Fig. 2 displays the fractional surface coverage of Mn^{2+} ions at both the $\{001\}$ and $\{210\}$ surfaces as a function of the overall mole fraction of Mn^{2+} , X_{Mn} , present in the film over a range of temperatures. Due to the finite thickness of the film, it is problematic to define a so-called ‘bulk’ composition and we have found it more useful to plot quantities of interest as a function of the total mole fraction of Mn^{2+} . The straight lines in Fig. 2 indicate the behaviour expected if there were no segregation to or from the surface. For both thin films the surface concentration of Mn^{2+} increases sharply as a function of overall concentration, with enrichment of the surface layer by

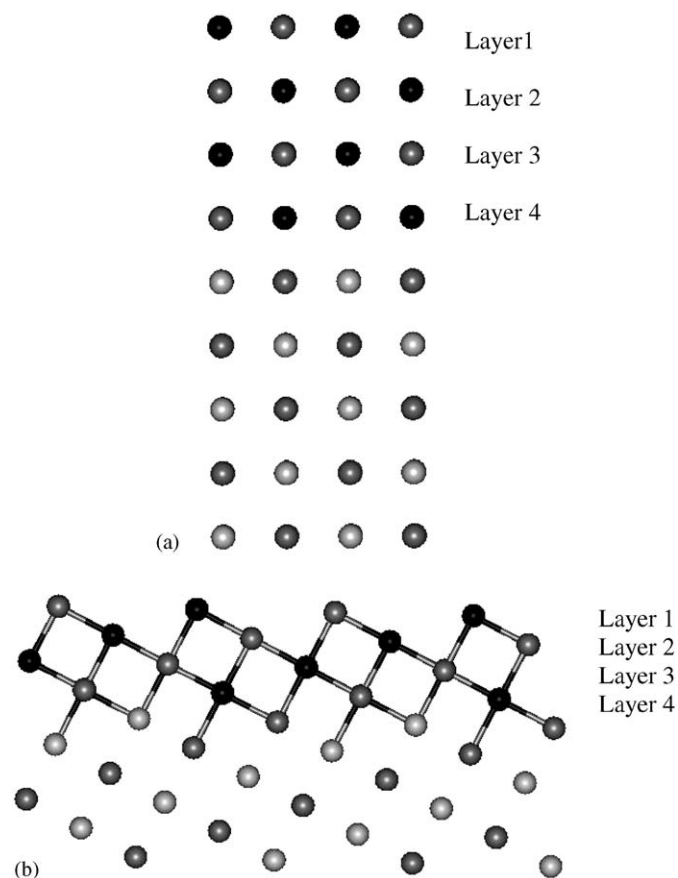


Fig. 1. The stacking sequences and the surface unit cells of the MgO (a) $\{100\}$ and (b) $\{210\}$ thin films. For clarity, the cations of the substrate are light grey and the cations of the thin film in black. The labels illustrate the numbering scheme employed for describing the surface layering of each cell.

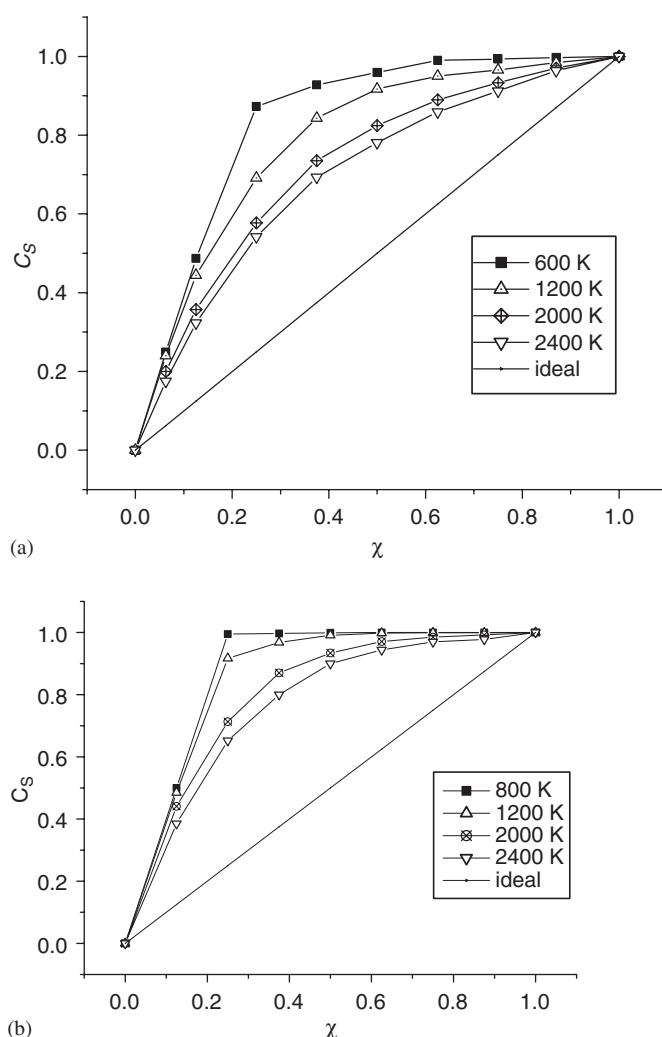


Fig. 2. The fractional surface coverage of Mn^{2+} ions plotted as a function of the overall Mn^{2+} mole fraction x of the thin film at different temperatures for the (a) $\{100\}$ and (b) $\{210\}$ surfaces.

the larger Mn^{2+} ion at all temperatures for all compositions. For a given composition, the surface concentration of Mn^{2+} ions for the $\{210\}$ surface is greater than that for the $\{100\}$ termination and at 600 K almost all the Mn^{2+} ions are at the surface. Indeed, the surface concentration of Mn^{2+} ions is greater at all temperatures and compositions for the $\{210\}$ termination (this is illustrated for calculated surface concentrations at 800 K in Fig. 3). The surface concentration varies with temperature, as also clearly shown in Fig. 2 (and Fig. 4), with a decrease in the surface enrichment by Mn^{2+} with increasing temperature, consistent with the increasing (configurational) entropy contribution to the free energy of mixing driving the Mn^{2+} back into the film. This decrease in surface enrichment is greater for the $\{001\}$ thin film.

An important difference in the behaviour of the two thin films is observed on examination of the ratio $\text{Mn}^{2+}:\text{Mg}^{2+}$ as a function of depth, which is displayed in Fig. 4 for an overall 50:50 composition. For the $\{001\}$ thin film the ratio decreases rapidly with depth. In contrast, the $\text{Mn}^{2+}:\text{Mg}^{2+}$ ratio for the $\{210\}$ thin film tends to be very similar for layers 2 and 3. This similarity in the $\text{Mn}^{2+}:\text{Mg}^{2+}$ ratio for layers 2 and 3 tends to increase with temperature, as the configurational entropy term drives Mn^{2+} ions back into the interior.

In Fig. 5, we display representative snapshots of the surface structure at 800 K for total Mn^{2+} mole fractions $x = 0.25$ for both surface terminations (Fig. 5). At the $\{100\}$ surface the surface occupancy by Mn^{2+} is 0.87 and the remaining Mg^{2+} ions tend to form chains along the $[110]$ direction (Fig. 5a). For overall compositions with x greater than 0.375 the surface cations are almost all Mn^{2+} . At 2400 K the surface coverage is reduced to 0.54, and in contrast to the 800 K results, the Mg^{2+} ions at the surface

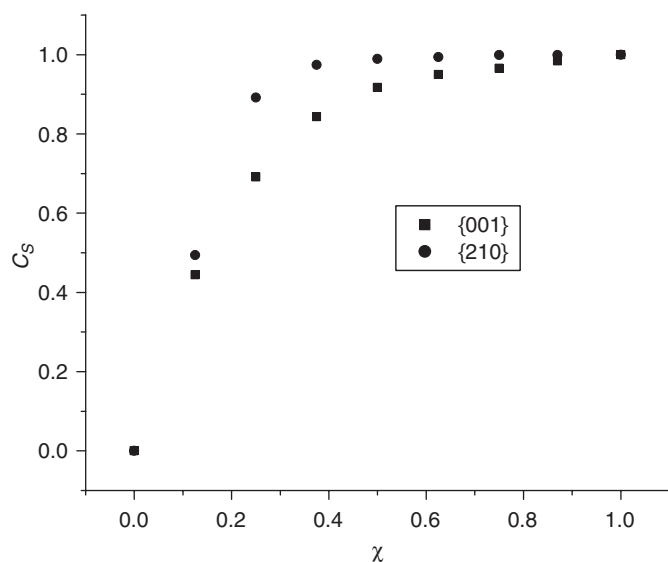


Fig. 3. Comparison of the fractional coverage for the $\{001\}$ and $\{210\}$ thin films at 1200 K, as a function of the overall Mn^{2+} mole fraction x of the thin film.

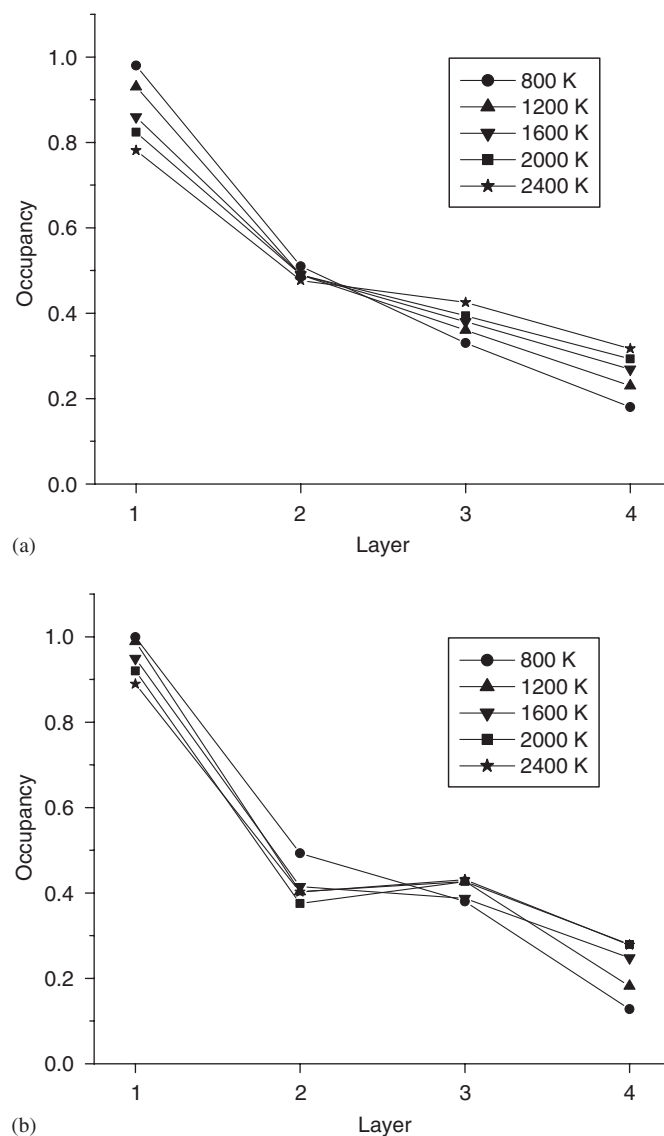


Fig. 4. The fractional occupancy of Mn^{2+} ions in the four layers of the films as a function of depth and temperature for (a) $\{100\}$, (b) $\{210\}$ -terminated films. The example shown is for a 50:50 mixture. Layer 1 is at the surface and layer 4 directly above the substrate.

form islands, with the Mn^{2+} forming chains along the $[110]$ direction (Fig. 5b). For the $\{210\}$ surface at 800 K the surface occupancy of Mn^{2+} ions is almost 1.0 and most of the Mn^{2+} ions are in the outermost layer. At 1600 K the surface coverage of Mn^{2+} ions has reduced so that some of the Mn^{2+} ions occupy positions within the interior of the film (Fig. 5c).

As we have discussed previously, the surface of a crystal or thin film always provides a different elastic and electrostatic environment to that of the bulk, and impurities/defects are thus driven to or from the surface. A convenient description of this is given by a segregation isotherm. This is frequently assumed to be of the Langmuir form [22] such that for a system containing two species, A and B, and a bulk concentration of species A, c , the surface concentration c_s of species A varies with temperature, T ,

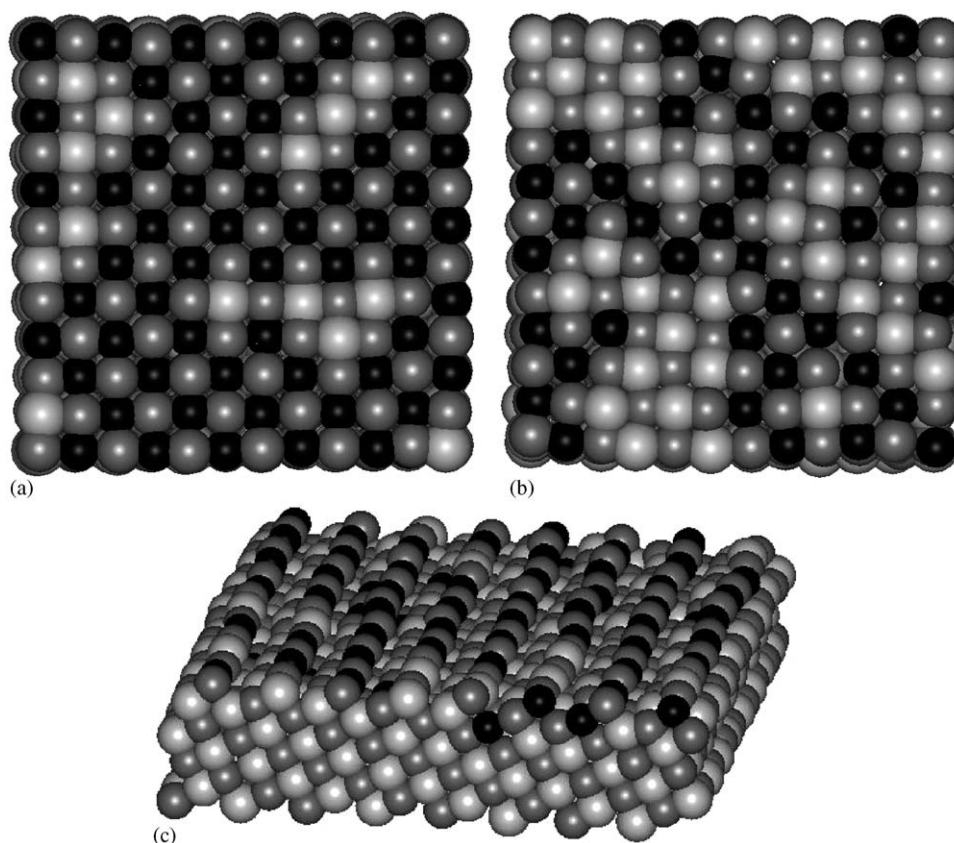


Fig. 5. Snapshots of the surface structure for a total Mn mole fraction $x = 0.25$ for (a) $\{100\}$ surface at 800 K, (b) $\{100\}$ surface at 2400 K and (c) $\{210\}$ surface at 1600 K. Dark grey, light grey and black represent oxygen, magnesium and manganese ions, respectively.

according to

$$\frac{c_s}{1 - c_s} = \frac{c}{1 - c} \exp\left(-\frac{\Delta H^{\text{seg}}}{k_B T}\right), \quad (1)$$

where ΔH^{seg} is a temperature and coverage-independent enthalpy of segregation [20]. Surface and bulk atomic ratios (A:B), x_s and x_b , are given by $c_s/(1 - c_s)$ and $c/(1 - c)$, respectively. We define the surface as the outermost layer (i.e., layer 1 in Fig. 1) and the bulk as the remaining layers (i.e., layers 2–4 in Fig. 1). Experimental enthalpies of segregation are conventionally extracted from plots of the logarithm of the surface atomic ratio versus $1/T$.

Fig. 6 plots the logarithm of the ratio of the surface atomic ratio to the total atomic ratio (i.e., $\ln(x_s/x_b)$) against the reciprocal temperature. The linear plots for a given total film composition (fixed x) suggests that, despite the somewhat non-uniform distribution of Mn^{2+} ions over the inner layers of the film shown in Figs. 4a and b, the overall segregation behaviour in each film is still given to a good approximation by an equation of Langmuir type (Eq. (1)), where c on the right-hand side of this equation is no longer the bulk concentration but the mean concentration in the interior of the film. We have determined, for each composition, a value of the effective heat of segregation, ΔH^{seg} , which we define as that obtained from the slope of a line fitted to the data points for a given composition in Fig. 6. The values of ΔH^{seg} are displayed in Figs. 7a and b as a

function of the total Mn^{2+} concentration for the $\{100\}$ and $\{210\}$ surfaces, respectively. The graph demonstrates that ΔH^{seg} varies strongly with composition. The value of ΔH^{seg} for the $\{100\}$ film increases from -48 to -27 kJ mol^{-1} (i.e., the driving force for segregation decreases) in the range $x = 0.0625$ – 0.25 . The variation at higher values of x is smaller and $\Delta H^{\text{seg}} \approx 30 \text{ kJ mol}^{-1}$ for $x > \approx 0.2$. There is some hint of a further decrease in the magnitude of ΔH^{seg} at the highest Mn concentrations, where the surface coverage is close to a complete monolayer. Overall the enthalpy of segregation varies by a factor of approximately two with surface coverage. The value of ΔH^{seg} in the $\{210\}$ films is more negative than those for $\{100\}$ films and the driving force of segregation is greater, which is expected from the surface occupation of Mn^{2+} ions in Figs. 2–4. Again ΔH^{seg} is strongly dependent on composition; the value of ΔH^{seg} increases from -65 kJ mol^{-1} at $x = 0.0625$ to -48 kJ mol^{-1} at $x = 0.5$. For concentrations greater than $x = 0.5$, ΔH^{seg} decreases to a value of -57 kJ mol^{-1} .

For comparison, values of ΔH^{seg} of -44.4 to -80 kJ mol^{-1} have been determined for $\{100\}$ surfaces of $\text{Ca}_x\text{Mg}_{1-x}\text{O}$ using a number of experimental methods for bulk concentrations between 180 and 220 ppm [21]. In addition, calculated values [5] for $\text{Ca}_x\text{Mg}_{1-x}\text{O}$ lie between -105 kJ mol^{-1} for point defects (dilute limits in both the bulk and at the surface) and at -40 kJ mol^{-1} for a

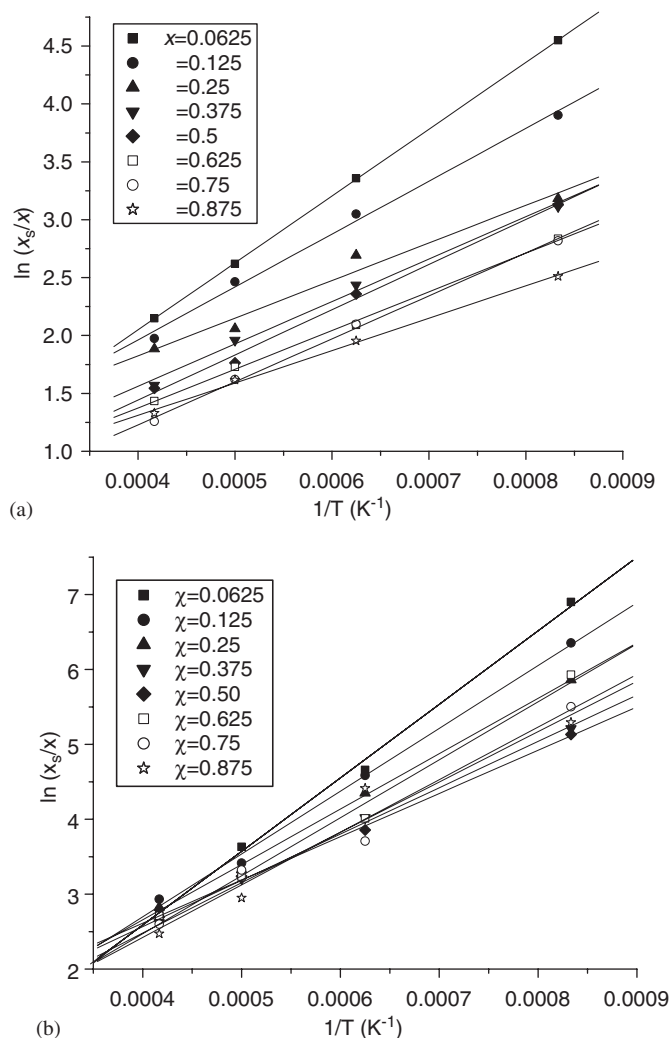


Fig. 6. Logarithm of the ratio of the surface atomic ratio of Mn^{2+} to the total atomic ratio (i.e., $\ln(x_s/x_b)$) as a function of reciprocal temperature for (a) {100} and (b) {210} thin films, respectively. The lines represent a linear fit to the calculated values.

fractional surface coverage of 1.0 [22]. These calculations were on dilute systems in contrast to our present calculations. Our results for ΔH^{seg} of approximately -30 kJ mol^{-1} for a smaller impurity cation at the {100} surface (Mn^{2+} as opposed to Ca^{2+}) are thus not unreasonable. Variations in ΔH^{seg} with surface termination have been noted previously in static lattice calculations [23]. To a first approximation this variation reflects the larger difference between the {210} surface energies of the two binary oxides (2.3 and 1.7 J m^{-2} for MgO and MnO , respectively) compared with that between the {100} energies (1.3 J m^{-2} and 1.0 J m^{-2} , respectively).

Thus at all compositions Mn^{2+} segregates to the surface, consistent with the smaller {001} and {210} surface energies of MnO relative to that of MgO . If the enthalpy of segregation of Mn^{2+} were both temperature and coverage independent, then all the points in Fig. 6 would lie on the same straight line; the form of the actual plot is consistent with a marked variation with coverage. The enthalpy of

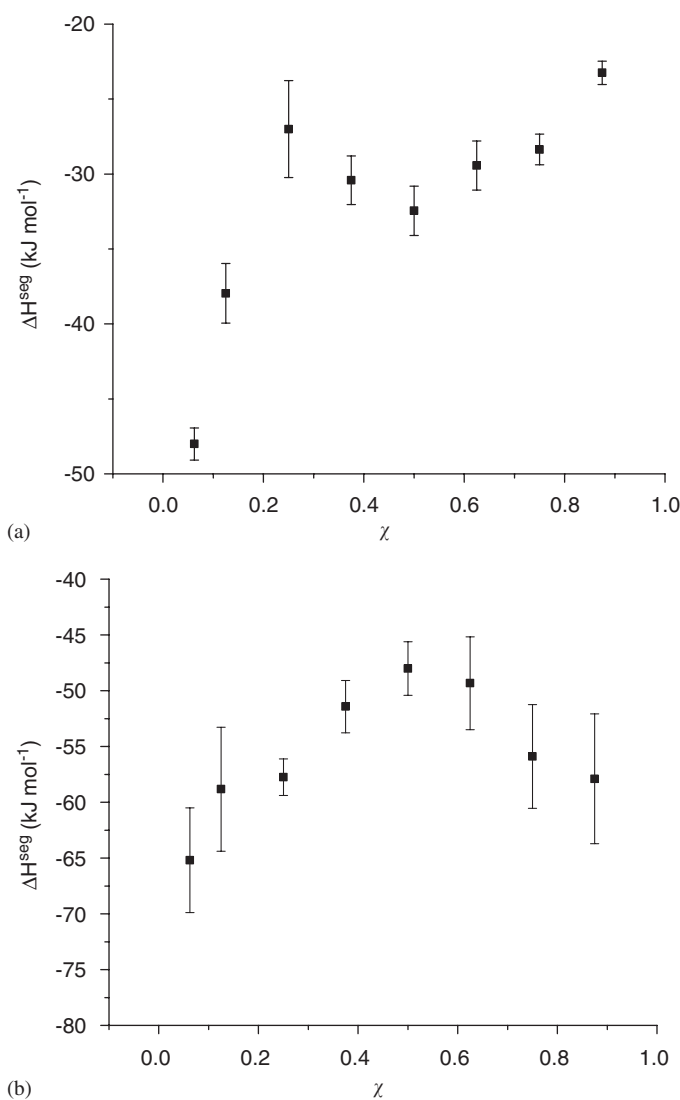


Fig. 7. Calculated values of ΔH^{seg} plotted as a function of the total Mn^{2+} atomic ratio for (a) {100} and (b) {210} thin films. The values of ΔH^{seg} are determined from the linear fit to the data in Fig. 6. The error bars are derived from the uncertainties in the fit and the differences obtained in the four consecutive simulations.

segregation for the lowest total concentrations of Mn^{2+} is larger than at higher concentrations, reflecting the larger release of strain accompanying the segregation at low Mn^{2+} concentrations which leaves the interior of the film largely Mn^{2+} free. Increasing the temperature leads to larger Mn^{2+} concentrations in the interior consistent with configurational entropy arguments.

4. Conclusions

We have employed the MCX technique to calculate directly the surface concentration of MnO/MgO thin films on a MgO substrate as a function of temperature and bulk composition. At all concentrations, the surface is Mn -rich; the lower surface energies of MnO dominates the energetics even when the film is Mn -rich and segregation of Mg would

reduce the strain energy in the interior of the film. The depth profile while showing overall a decrease in the concentration of Mn^{2+} ions with depth is somewhat different for the {210} than for the {100} film. At high temperatures, the Mn^{2+} ions are more dispersed throughout the film. The Langmuir isotherm, of the form of Eq. (1), has been shown to provide a useful approximation for the calculation of the enthalpy of segregation. We stress the effective enthalpy of segregation is strongly dependent on the total Mn^{2+} mole fraction, and varies from one surface to another. However, the Langmuir–McClean theory neglects the less-marked segregation to layers other than the outermost (but which is evident from Fig. 4), and the non-ideality of the bulk solid solution. To describe segregation in oxide solid solutions, including the segregation in the layers immediately under the surface layer will require the formulation of suitable non-Langmuir isotherms (cf. Ref. [22]).

References

- [1] W.C. Mackrodt, C. Noguera, N.L. Allan, Faraday Discuss. 114 (1999) 105.
- [2] R.E. Bailey, S. Nie, J. Am. Chem. Soc. 125 (2003) 7100.
- [3] D.C. Sayle, R.L. Johnston, Curr. Opin. Solid State Mater. Sci. 216 (2003) 3.
- [4] D.J. Harris, J.H. Harding, M. Lavrentiev, N.L. Allan, J.A. Purton, J. Phys.: Condens. Matter 16 (2004) L187.
- [5] J.A. Purton, G.D. Barrera, M.B. Taylor, N.L. Allan, J.D. Blundy, J. Phys. Chem. B 102 (1998) 5202.
- [6] M.Y. Lavrentiev, N.L. Allan, G.D. Barrera, J.A. Purton, J. Phys. Chem. B 105 (2001) 3594.
- [7] I.T. Todorov, N.L. Allan, M. Yu. Lavrentiev, C.L. Freeman, C.E. Mohn, J.A. Purton, J. Phys.: Condens. Matter 16 (2004) S2751.
- [8] P.W. Tasker, E.A. Colbourn, W.C. Mackrodt, J. Am. Ceram. Soc. 68 (1985) 74.
- [9] W.C. Mackrodt, P.W. Tasker, Mater. Res. Soc. Symp. Proc. 60 (1986) 291.
- [10] M.J. Davies, P. Kenway, P.J. Lawrence, S.C. Parker, W.C. Mackrodt, P.W. Tasker, J. Chem. Soc. Faraday Trans. 2 85 (1989) 555.
- [11] P.R. Kenway, S.C. Parker, W.C. Mackrodt, Surf. Sci. 326 (1995) 301.
- [12] C.C. Battaille, R. Najafabadi, D.J. Srolovitz, J. Am. Ceram. Soc. 78 (1995) 3195.
- [13] J.A. Purton, M.Yu. Lavrentiev, N.L. Allan, I.T. Todorov, Phys. Chem. Chem. Phys. 7 (2005) 3601.
- [14] C.R.A. Catlow, W.C. Mackrodt (Eds.), Computer Simulation of Solids, Springer, Berlin, 1982 (p. 3, Chapter 1).
- [15] [a] D. Parry, Surf. Sci. 49 (1975) 433;
[b] D. Parry, Surf. Sci. 54 (1976) 195.
- [16] G.V. Lewis, C.R.A. Catlow, J. Phys. C 18 (1985) 1149.
- [17] N.L. Allan, G.D. Barrera, R.M. Frachia, M. Yu. Lavrentiev, M.B. Taylor, I.T. Todorov, J.A. Purton, Phys. Rev. B 63 (2001) 094203.
- [18] B.J. Wood, R.T. Hackler, D.P. Dobson, Contrib. Mineral. Petrol. 115 (1994) 438.
- [19] N.I. Metropolis, A.W. Rosenbluth, M.N. Rosenbluth, A.H. Teller, E. Teller, J. Chem. Phys. 21 (1953) 1087.
- [20] G. Tréglia, B. Legrand, F. Ducastelle, A. Saúl, C. Gallis, I. Meunier, C. Mottet, A. Senhaji, Comput. Mater. Sci. 15 (1999) 196.
- [21] R.C. McKune, P. Wynblatt, J. Am. Ceram. Soc. 66 (1983) 111;
R.C. McKune, R.C. Ku, in: W.D. Kingery (Ed.), Advances in Ceramics, vol. 10, American Ceramic Society, Columbus, OH, 1984, p. 217.
- [22] W.C. Mackrodt, P.W. Tasker, J. Am. Ceram. Soc. 72 (1989) 1576.
- [23] P.R. Kenway, P.M. Oliver, S.C. Parker, D.C. Sayle, T.X.T. Sayle, J.O. Titiloye, Mol. Sim. 9 (1992) 83.